

Studies of Multipass Beam Breakup and Energy Recovery Using the CEBAF Injector Linac

N. S. Sereno and L. S. Cardman †

Nuclear Physics Laboratory and Department of Physics
University of Illinois at Urbana-Champaign, Champaign, Il. 61820,
G. A. Krafft, C. K. Sinclair, and J. J. Bisognano ‡
Continuous Electron Beam Accelerator Facility
12000 Jefferson Avenue, Newport News, Va 23606-1909



Abstract

Beam breakup (BBU) instabilities in superconducting linacs are a significant issue due to the potentially high Q values of the cavity higher order modes (HOMs). The CEBAF accelerator, which employs high CW current and 5-pass recirculation through two superconducting linacs, poses unique instability problems. An experimental investigation of multipass BBU along with energy recovery has been completed using a single recirculation through the CEBAF injector linac. Experimental results are compared with computer simulation of multipass BBU.

I. INTRODUCTION

Multipass BBU is characterized by a maximum current (threshold current) above which beam loss occurs. The threshold current is the maximum average current at which the power deposited by the beam into the HOM equals the power dissipated by the HOM through resistive losses. The threshold current for the most unstable mode is the maximum beam current that can be accelerated without beam loss. The HOM Q parameterizes the mode losses and can be the same order of magnitude as the fundamental mode Q (10^9 – 10^{10}). The CEBAF/Cornell cavity design incorporates HOM damping thereby reducing HOM Q values to the range 10^4 – 10^5 [1]. As a result, BBU threshold currents for the full CEBAF linac are calculated to be between 10 and 20 mA [2]—two orders of magnitude above the maximum design current of 200 μ A.

The CEBAF/Cornell cavity design was tested under the conditions of both acceleration and energy recovery of the second-pass beam in the CEBAF injector. The injector offered worst-case conditions (lowest threshold currents) for multipass beam breakup because of the low injection energy of 5.5 MeV (as opposed to the nominal 45 MeV for the full CEBAF linac), the ability to produce in excess of 200 μ A CW current, and the ability to change the transverse optics of the recirculation path to lower the threshold current. The fact that no evidence for multipass beam breakup was experimentally observed for both second-pass

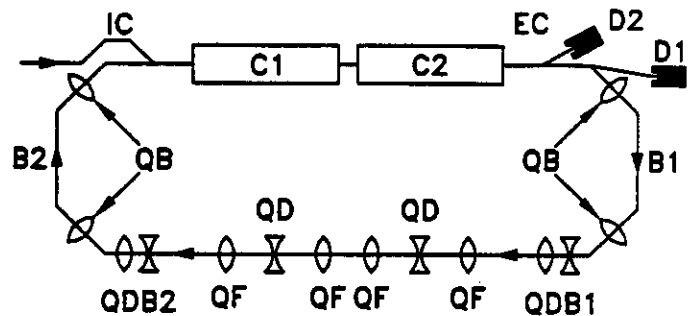


Figure 1: Recirculator layout.

acceleration and energy recovery under these-worst case conditions indicates that the HOM damping incorporated in the CEBAF/Cornell cavity design is entirely adequate to prevent multipass BBU in the full CEBAF linac.

II. RECIRCULATOR DESCRIPTION

Figure 1 shows schematically the CEBAF injector linac including the beam recirculation path. The linac consists of two cryomodules C1 and C2, each containing eight 5-cell, 1497 MHz superconducting cavities. The beam is injected into the linac at 5.5 MeV and accelerated to 42.8 MeV after C2. The beam is bent 180° by B1, travels to B2 where it is bent by another 180° and arrives back on the linac axis. Finally it is combined with the injected beam on the linac axis by injection chicane IC and is either accelerated to 80 MeV and dumped at D1 or decelerated to 5.5 MeV and dumped at D2 after the energy recovery chicane EC, which separates the first-pass accelerated beam from the low-energy second-pass beam. Path length adjustment was accomplished by mounting B1 on a movable platform which could be translated along the linac axis by ~ 10 cm ($1/2$ of an RF wavelength at 1497 MHz).

III. TRANSVERSE OPTICS

The recirculation arc transverse optics provided both dispersion-free beam transport and independent adjustment of both x and y plane optics. B1 and B2 were designed to be doubly achromatic in the horizontal plane. Two quadrupoles per bend (QBs) were used to set the

†Supported by N.S.F grant #PHY-89-21146

‡Supported by D.O.E. contract #DE-AC05-84ER40150

Frequency (MHz)	R/Q (Ω)	Q
1899.6	21.9	*90,000
1969.6	48.1	4,000
2086.9	13.1	10,000
2110.5	25.6	*30,000

Table 1: HOM parameters (* from RF measurement).

dispersion and its slope to zero after the bend. Doublets QDB1 and QDB2 were used to match the beam out of B1 and into B2 respectively. The six quadrupoles QD and QF formed a FODO structure that was adjusted to provide various optical settings. As the six quadrupoles were varied the optics of the rest of the recirculator was left unchanged during the experiment. Setting 1 was simply a negative identity matrix (-I) transfer in both x and y planes across the FODO array. For settings 2–4 the y plane optics was changed and the x plane was kept at -I. Settings 5 and 6 were achieved by reversing the polarity of the quads for settings 1 and 2, which resulted in x being varied and y remaining -I. The energy recovery setting was identical to setting 1 except that doublet QDB2 was re-adjusted to provide the smallest beam spot possible at D2.

Calculations of the transverse optics were performed using the code DIMAD. Beam transport calculations were performed for all optical settings including energy recovery. In addition, quadrupole strengths of doublets QDB1 and QDB2 were fit to measurements of the M_{12} and M_{34} matrix elements measured before C1, between C1 and C2 and after C2 for each optical setting. A cavity model was incorporated into DIMAD (and the BBU code TDBBU [2]) which included the cavity focussing by the fundamental accelerating mode at low energy. The calculations did not take into account the small x - y coupling observed at the low energies in the injector [3].

IV. ENERGY RECOVERY

Superconducting cavities have the advantage that high gradients can be maintained under CW operating conditions because of low wall losses. If a beam is decelerated, efficient conversion of beam energy to fundamental mode field energy is possible. Energy recovery of a FEL beam driven by a superconducting linac by means of recirculation is a possible way of greatly increasing the efficiency of the laser since most of the beam energy remains after lasing occurs [4]. The CEBAF energy recovery experiment extended previous experiments [5], [6], [7] to the relatively high gradients (5 MV/m) of CEBAF cavities. In the experiment, the second pass beam was decelerated to 5.5 MeV (at up to 30 μ A CW current) indicating full energy recovery within the 1.8% energy measurement uncertainty.

V. BEAM BREAKUP SIMULATIONS

Setting	I_t (mA)	I_m (μ A)
1	5.3	215
2	6.3	68
3	19.5	120
4	13.2	95
5	15.5	64
6	5.0	67
Energy recovery	.4	30

Table 2: Threshold current and maximum beam current attained for each optical setting.

The beam breakup simulations were performed using the code TDBBU for all optical settings including energy recovery. The cavity HOMs were treated as high Q uncoupled resonators with a strength given by the shunt impedance R/Q . These modes deflect the beam in either the x or y plane. Table 1 lists parameters of the HOMs used in the simulations; the asterisk indicates the Q values for these modes come from RF measurements described in the next section. Reference [1] lists the shunt impedance in terms of the parameter Z'' , which is given by $R/Q = (Z''/Q)(l_e/k^2)$ where k is the HOM wavenumber and l_e is the effective length of the HOM in the cavity (0.5 m). Finally, the code uses the first-order transfer matrix describing the recirculation path from the end of C2 to the beginning of C1 as computed using DIMAD.

Table 2 lists the threshold current I_t computed for each optics setting along with the maximum CW current I_m achieved in the experiment. Similar BBU calculations for the full CEBAF linac indicate threshold currents in the range 10–20 mA [2] so that the injector recirculator is calculated to be more sensitive to multipass BBU by a factor of 2 in the threshold current. For setting 1, over 200 μ A CW was recirculated. This is the CEBAF maximum design current, but is still an order of magnitude below the calculated threshold current for setting 1. The energy recovery setting is seen to have the lowest calculated threshold current due to large recirculation transfer matrix elements. Beam current was primarily limited by large beam sizes on the second pass (with energy recovery having the largest) that resulted in scraping. The beam loss monitoring system shut the beam off when approximately 1 μ A of scraping occurred.

VI. RF MEASUREMENTS

An additional experiment was performed to externally excite the HOMs using an RF kicker that deflected the beam transversely. Figure 2 shows schematically the RF HOM measurement that was performed using a recirculated CW beam. A broadband stripline kicker operating between 350 and 650 MHz was used to deflect the beam transversely. Signals at a particular HOM frequency were detected using the last cavity of C2. Aliasing of the kicker signal by the

Network Analyzer

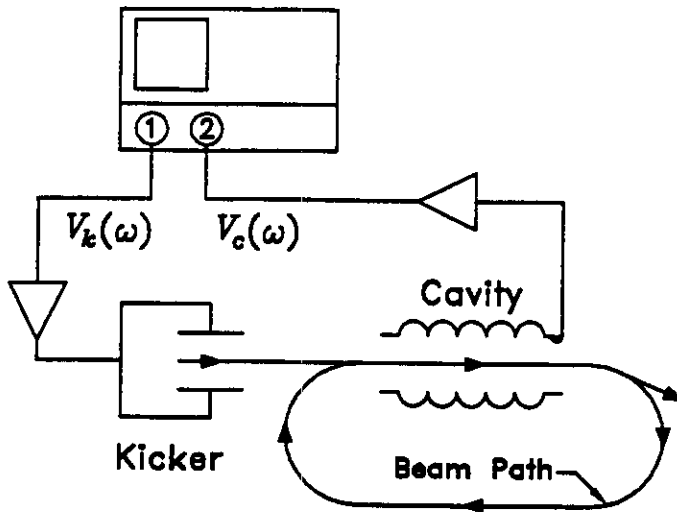


Figure 2: RF HOM measurement schematic.

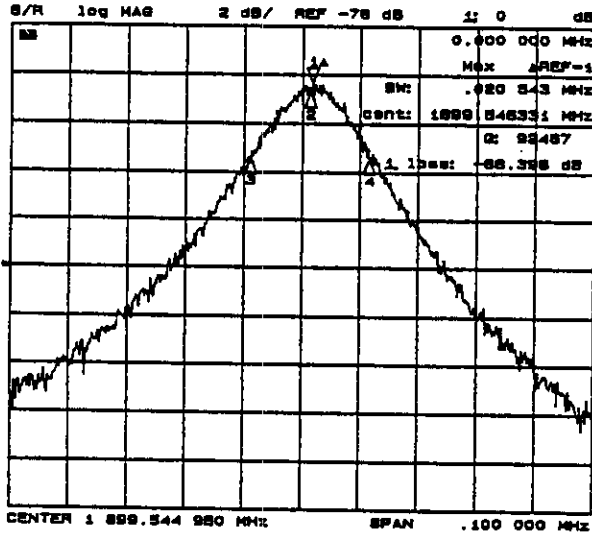


Figure 3: 1899 MHz HOM at 99 μ A CW beam current.

bunching frequency insured that HOMs near 2 GHz were excited. Under recirculation conditions the cavity signal V_c is given in terms of the kicker drive signal V_k by

$$\frac{V_c(\omega)}{V_k(\omega)} = \mathcal{F} \frac{IZ(\omega)}{1 - I/I_t} \quad (1)$$

where $Z(\omega)$ is the total transverse impedance due to all the cavity HOMs and \mathcal{F} is an overall scale factor. The formula shows instability occurring at a particular threshold current. Far from threshold for a particular HOM, the ratio in equation 1 is simply a linear function of the current with the slope proportional to the mode impedance.

Figure 3 shows the 1899 MHz HOM measured using the setup in figure 2. The network analyzer was set up to measure S_{21} (the ratio in equation 1) where port 1 was used to drive the kicker and port 2 was used to detect the cavity signal. For both HOMs measured (at 1899 and

2110 MHz) the height of the peak was plotted as a function of the beam current I for all optical settings including energy recovery. No significant deviation from linearity was observed—a result consistent with the computed threshold currents in table 2.

VII. CONCLUSIONS

From experimental and simulation results, multipass BBU did not prevent high-current operation of the injector recirculator. The main limitation on recirculated current was scraping, primarily due to non-ideal matching of the second-pass beam out of B2. The results indicate that the full CEBAF linac should not be susceptible to multipass beam breakup at the maximum design current of 200 μ A. An FEL driven by a linac that uses energy recovery to increase efficiency would need to incorporate careful optical design aimed at reducing second-pass spot sizes and increasing multipass BBU threshold currents.

ACKNOWLEDGMENTS

The authors express their gratitude to the CEBAF staff and especially to the members of the operations group who put in many long hours during these experiments. We also thank W. Barry who designed and prototyped the stripline kicker used in the RF measurement.

REFERENCES

- [1] J. C. Amato, *Identification and Analysis of TM111 and Schwettmann Cavity Modes*, SRF-850303-EX, (1984).
- [2] G. A. Krafft, J. J. Bisognano, S. Laubach, "Beam Breakup in Superconducting Linear Accelerators," (To be submitted to *Particle Accelerators*).
- [3] M. Tiefenback, Z. Li, L. Merminga, B. Yunn, "Emitance Measurements and Transverse Cavity Transfer Matrix in the CEBAF Nuclear Physics Accelerator," these proceedings.
- [4] R. Rohatgi, H. A. Schwettman, and T. I. Smith, "A Compact Energy Recovered FEL for Biomedical and Material Science Applications," *Proceedings of the 1987 Particle Accelerator Conference*, 230 (1988).
- [5] D. W. Feldman *et al.*, "The Los Alamos Free-Electron Laser Energy-Recovery Experiment," *Proceedings of the 1987 Particle Accelerator Conference*, 221 (1988).
- [6] G. R. Neil, J. A. Edighoffer, and S. W. Fornaca, "Superconducting Linac FEL Technology," *Proceedings of the Beijing FEL Seminar*, 232 (1989).
- [7] T. I. Smith, *et al.*, "Development of the SCA/FEL For Use in Bio-Medical and Material Science Experiments," *Proceedings of the 1986 International FEL Conference*, (1986).